METHYLENE BLUE REMOVAL BY PHASE SEPARATED POROUS GLASS

Emre Burak ERTUŞ [1], Çekdar Vakıf AHMETOĞLU [2], Abdullah ÖZTÜRK[3]

[1] Department of Mechanical Engineering, KTO Karatay University

[2]Materials Science and Engineering, İzmir Institute of Technology

[3] Metallurgical and Materials Engineering, Middle East Technical University

Keywords: Porous glass, Methylene Blue, Adsorption.

Abstract

In this study, it was aimed to utilize Porous glass (PG) as an adsorbent in MB removal from wastewater. PG powders were produced by melting and phase separation of an alkali borosilicate glass followed by selective leaching in HCl and an additional alkali treatment. The scanning electron microscope and N_2 adsorption/desorption techniques were applied to characterize the pore architecture of the PGs. Methylene blue (MB) adsorption efficiency was investigated from the change in MB concentration in the MB aqueous solutions with various concentrations through the absorbance of the solution at a wavelength of 664 nm monitored on a UV-Vis spectrometer. Results showed that the structure and textural properties of PG was evidently altered via alkali treatment hence affected its adsorption performance. The maximum adsorption capacity for alkali treated PG in the concentration ranges studied was 60.6 mg/g. The isotherm analysis indicated that the equilibrium data were well fitted to the Freundlich isotherm model.

1. Introduction

The usage of dyes in textile and chemical industry generates colored wastewaters, which often cause significant environmental problems. The dye-containing runoffs are hazardous for the biological stability of neighboring ecosystems and can be carcinogenic and mutagenic. Methylene blue (MB) is a cationic dye and commonly used for dying cotton, silk, and wood. MB can have various harmful effects on human being and animals [1]. Several methods including chemical oxidation [2], biodegradation [3], flocculation–coagulation [4], and adsorption [5] are available for the removal of dyes from industrial wastewaters. Among them, adsorption is a comparatively cheap and effective method in the removal of dyes from wastewaters [5].

So far, the most popular adsorption materials are activated carbon, clays, and agricultural solid wastes [6]. Among these adsorbents, phase separated PG is distinguished from other porous solids by its distinctive sponge-like interconnected porous structure, suitability for low cost mass production, reusability of waste glass, and mechanical integrity [7, 8]. Pore topology, volume, size, the surface area can be tailored via processing parameters [7]. PGs are produced in a variety of forms such as powder, beads, monoliths, fibers, or tubes. It is also known that PG does not cause catalyst poisoning. [9, 10]. Several studies have investigated the adsorption properties of PG. Kuznetsova et al. [11] examined the adsorption of iron ions by PG in diluted solutions of iron(III) chloride. Zhang et al. [12] studied the MB adsorption performance of polyvinylidene fluoride (PVDF)/porous glass composite membrane. To the best of the authors knowledge, no study has been reported on the MB adsorption behavior of phase separated PG.

The purpose of this study was to evaluate the MB adsorption performance and to analyze equilibrium adsorption isotherms of phase separated PG.

2. Experimental Procedure

2.1. Porous glass preparation

Porous glasses (PGs) were produced in accord with our previous study. Readers are referred to reference [13] for the details in the production. A sodium borosilicate glass with nominal composition of $55.7SiO_2$-$33.6B_2O_3$-$9.2Na_2O$-$1.5Al_2O_3$ (wt%) was produced by conventional melt-quenching technique using an electric furnace. To provide phase separation, the as cast glass was heat treated at 525 °C for 9 h. Later, the heat-treated glass pieces were acid leached using 1M HCl solution at 80 °C for 24 h. To remove the silica clusters precipitated in the pore channels, the acid leached porous glass (PG1) was additionally alkaline leached at room temperature using 0.5M NaOH solution for 2 h (PG2). After each leaching process, PGs were washed with distilled water and after all dried at 200 °C for 3 h. These modifications were followed to induce different pore architecture, surface

functionality and to observe their effect on the MB adsorption efficiency. All crushed and ground in an agate mortar with pestle. Finally, the resulting material was sieved in the size of less than 28 μm (500 mesh).

2.2 Characterization

The pore characteristics of PGs were measured via nitrogen (N_2) adsorption desorption method using Quantachrome Autosorb-6 instrument. Prior to the measurement, the PGs were evacuated at 200 °C for 3 h. Brunauer–Emmett–Teller (BET) equation was used to calculate the specific surface areas from the adsorption isotherm. The total pore volume was obtained from the amount of gas adsorbed at the relative pressure P/P_0= 0.99. The desorption branch of the nitrogen sorption isotherm was used to determine pore size distributions of PGs according to the BJH (Barrett, Joyner, Halenda) method, depended on the Kelvin equation, which relates the pore size with critical condensation pressure assuming a straight cylindrical pore model [14]. The structure of the pores was investigated by a scanning electron microscope (FE-SEM, Nova Nanosem 430, Hillsboro OR, USA).

To evaluate the adsorption properties of PGs Methylene Blue (MB), a cationic dye, was used as the absorbed media. Before the experiments, 240 mg/L MB/ deionized water solution was prepared and diluted to the desired concentration. Adsorption tests were conducted in a glass container. 50 mg PGs and 50 mL MB solution (concentration between 20 and 240 mg/L with 40 mg/L increment) were added to the glass container than the mixture was magnetically stirred for an hour at room temperature. The suspension was centrifuged for 30 min at 4500 rpm and then supernatant was analyzed to determine MB adsorption change at the wavelength of 665 nm using a UV spectrophotometer (Agilent, Cary60). The concentration of MB was calculated referring to the calibration curve of MB. The amount of methylene blue uptake by PGs, q_e (mg/g) and the adsorption rate R (%) was calculated according to equations (1) and (2) respectively.

$$q_e = \frac{V(C_0 - C_e)}{W} \quad (1)$$

$$R = \frac{C_0 - C_e}{C_0} x100 \quad (2)$$

where V (L) is the volume of MB solution and W (mg) is the mass of PGs. C_0 and C_e (mg/L) are the initial and equilibrium concentrations of the MB in the solution, respectively. Freundlich [15] and Langmuir [16] equations were used to describe the equilibrium characteristics of adsorption, which are given in equations (3) and (4), respectively.

$$log q_e = log k_F + \frac{1}{n} log C_e \quad (3)$$

$$\frac{C_e}{q_e} = \frac{1}{k_L q_{max}} + \frac{C_e}{q_{max}} \quad (4)$$

In Freundlich equation, k_F ($(mg/m^2)(L/mg)^{1/n}$) is indicative of the adsorption capacity, and n (dimensionless) is the empirical parameter representing the energetic heterogeneity of the adsorption sites. For Langmuir type adsorption process q_{max} (mg/g) is the maximum monolayer adsorption capacity and k_L is a constant related to the energy of adsorption. The efficiency of the adsorption process could be predicted by the equilibrium parameter, R_L (dimensionless), using equation (5) [17].

$$R_L = \frac{1}{1 + C_0 K_L} \quad (5)$$

3. Results and Discussion

The N_2 sorption isotherms for PGs are shown in **Fig. 1(a).** The isotherms are of the Type IV(a) according to the IUPAC classifications, indicated that all glasses include mesoporosity. PGs exhibits the combination of H1 and H2 type hysteresis loop that is associated to pore-blocking/percolation in a narrow range of pore necks (ink-bottle pore model) or to cavitation-induced evaporation [14]. Isotherms exhibiting double hysteresis (two cycles) indicate a bimodal pore size distribution [18].

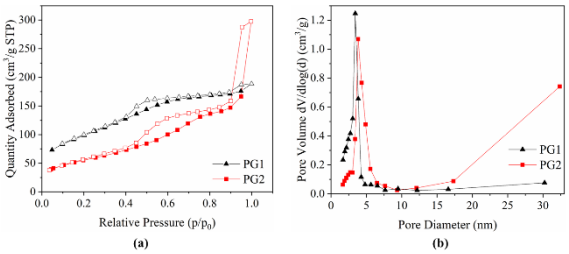

Figure 1. (a) N_2 adsorption-desorption isotherms, and **(b)** pore size distribution data for PGs.

The pore size distribution curves, shown in **Fig. 1(b)**, illustrate that the micro and mesopores coexists in PGs prepared, indicating that the pores formed hierarchical porosity. The pores around 4-5 nm are associated with the inter-particle spaces in between the channel walls and silica clusters (themselves as well). Also, the mesopores developed in a wider range up to 35 nm are related with the silica rich interconnected open-pore structure left behind the acid leaching what is called "liquation channels" [19, 20]. As a result of the following alkali treatment the size of the pores in the mesoporous range further increased, also some of the micropores diminished due to particle and/or surface dissolution of silica clusters [21].

The pore volume (Vp) and the specific surface area (SSA) values as calculated from N2 adsorption-desorption analysis for PG1 and PG2 were listed in **Table 1**. Associated with the findings about pore

size alteration, the SSA of PG2 decreased while V_p increased relative to PG1, as a result of the removal of silica clusters and enlargement of liquation channels.

Table 1. The specific surface area (SSA) and total pore volume (Vp) of PGs.

Adsorbent	SSA (m^2/g)	Vp (cm^3/g)
PG1	350.6	0.291
PG2	199.0	0.459

Fig. 2 shows the SEM images taken from the surfaces of the PGs produced at a magnification of 100,000x. The characteristic "worm-like" porous structure observed in both PGs. The liquation channels were better distinguishable than pores derived from silica clusters. The liquation channels i.e., silica skeleton of the PG2 deformed and the pores grew because of alkali leaching, proving the results of the N_2 sorption analysis.

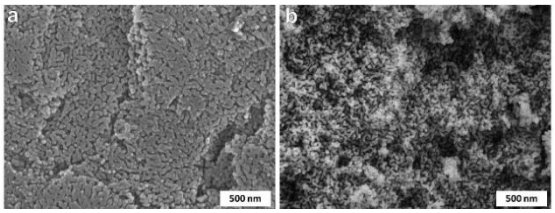

Figure 2. SEM images of **(a)** PG1 and **(b)** PG2.

Fig 3 (a) shows the relationship between initial MB concentration and the adsorption rate. At the initial MB concentration of 20 mg/L, PG2 exhibited higher adsorption rate (99.5%) than PG1 (60.1%). As the initial MB concentration was increased up to 240 mg/L, the adsorption rates of PG1 and PG2 decreased to 16.6% and 27%, respectively. It is related to the amount of active adsorption sites at PG pore walls. With increasing dye concentration, the active adsorption sides on the adsorbing surface become saturated with dye molecules [12]. Therefore, a decrease in the removal efficiency observed as the initial MB concentration increased. The adsorption rate for PG2 was higher than that for PG1 for all concentrations studied. As mentioned previously, removing the silica clusters by alkaline leaching increased the pore volume and enlarged the liquation channels. A higher adsorption rate for PG2 may be explained by easy diffusion of the aqueous MB solution through the porous structure and alteration of the surface functionality. That is, it is assumed that alkali treatment increased the surface adsorption sites or changed their nature, causing a superior adsorption performance. [22, 23].

Fig 3 (b) shows the nonlinear fitting of experimental adsorption data to the Freundlich and Langmuir models. The calculated values for the corresponding parameters are given in **Table 2**. According to correlation coefficient (R^2) it is suggested that the adsorption of MB on PGs is fitted well to both equations with R^2 values greater than 0.9. It can be considered that the adsorption is intermediate between Langmuir and Freundlich isotherm models. But, Freundlich isotherm model which has greater R^2 values was more suitable to describe this adsorption process. The better fit with the Freundlich model suggests that the adsorption process to be multilayer and the heterogeneity of active sites on the surface of the adsorbent i.e., the sites involved in the adsorption process were not in the same type. It is known that PGs have a negative surface charge and slightly acidic character due to silanol (Si-OH) groups on their surface [8]. MB adsorption is simply due to the electrostatic attraction between the negatively charged PG surface and the positively charged MB molecules in solution. In addition, the hydrogen bonding between the amine group of MB molecule with Si-OH groups on PG surface is effective [24]. The diversity of active groups on the surface of PG is thought to explain the heterogeneity. Surface active groups can be in the form of (i) isolated free silanol, (ii) geminal free silanol, and (iii) vicinal groups. Also, siloxane and borate groups can be formed on PG surface [8, 25]. Values of n between 1 and 10 implies favorable adsorption. For PG1 and PG2, n values are greater than 1 confirmed the favorably adsorption of MB on PGs and more favorable for PG2. On the other hand, 1/n values smaller than 1 in the Freundlich model, indicates a monolayer adsorption. The k_F value is a relative indicator of the adsorption capacity and PG2 has superior k_F than PG1 [25].

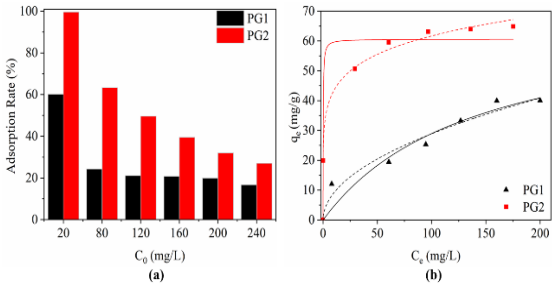

Figure 3. (a) The effect of initial MB concentration on adsorption rates of PGs and **(b)** equilibrium adsorption isotherms of MB onto PGs with simulations by Freundlich (dashed line) and Langmuir (solid line) isotherm models.

Table 2. Langmuir and Freundlich adsorption isotherm constants and correlation coefficients.

Adsorbent	**Langmuir model**			
	q_{max}	k_L	R_L	R^2
PG1	69.71±22.8	0.007	0.3731	0.93
PG2	60.69±2.31	5.9	0.0007	0.96
Adsorbent	**Freundlich model**			
		n	k_F	R^2
PG1		2.04	2.89	0.94
PG2		6.66	30.5	0.98

For Langmuir isotherm model, R_L value indicates the type of the isotherm as either unfavorable (R_L >1), linear (R_L = 1), irreversible (R_L= 0), or favorable (0 < R_L <1) [17]. Values of R_L were between 0 and 1 for PGs implying that the adsorption process was favorable. The R_L value of PG2 is very close to 0, suggesting a higher degree of irreversible adsorption than PG1. Also, the k_L value of PG2 indicates that MB has a higher interaction with PG2 than PG1. Although all other data show that the adsorption performance of PG2 is better than PG1, the calculated q_{max} value of PG2 (60.69±2.31 mg/g) was lower than PG1 (69.71±22.8 mg/g). It is considered that this calculation is not very reliable due to the high curve fit error value.

4. Conclusions

1. Hierarchically porous glasses (PGs) were produced by selective acid leaching processes conducted on a sodium borosilicate glass. The alkaline treatments have intense effects on the pore structure, the total pore volume increased (0.459 cm^3/g), and specific surface area decreased (199 m^2/g) with successive alkaline treatment.
2. Freundlich isotherm model was more suitable to describe MB adsorption process and the diversity of active groups on the surface of PG is thought to explain the heterogeneity of adsorption model.
3. R_L values between 0 and 1 for PGs implied that the adsorption process was favorable, that is related to the hierarchically (micro-meso) porous structure, high Vp, and SSA combined with the negatively charged silanol residues on the surface of this structure. The R_L value of PG2 is very close to 0, indicating a higher degree of irreversible adsorption than PG1 may be explained by easy diffusion of the aqueous MB solution through the porous structure and altered surface functionality.
4. The results obtained showed that the PGs are an appropriate adsorbent for removal of cationic dyes from aqueous solutions.

Acknowledgment

The authors thank Middle East Technical University for the partial financial support through project number BAP-03-08-2016-004.

References

1. Khan, S. and A. Malik, 2014, Springer. p. 55-71.
2. Dutta, K., et al., Journal of hazardous materials, 2001. **84**(1): p. 57-71.
3. Bharti, V., et al., Environmental research, 2019. **171**: p. 356-364.
4. Alizadeh, M., et al., Iranian Journal Of Chemistry And Chemical Engineering, 2015. **34**(1): p. 39-47.
5. Allen, S. and B. Koumanova, Journal of the University of Chemical Technology and Metallurgy, 2005. **40**(3): p. 175-192.
6. Rafatullah, M., et al., Journal of hazardous materials, 2010. **177**(1-3): p. 70-80.
7. Enke, D., F. Janowski, and W. Schwieger, Microporous and mesoporous materials, 2003. **60**(1-3): p. 19-30.
8. Schüth, F., K.S.W. Sing, and J. Weitkamp, *Handbook of porous solids*. 2002: Wiley-Vch.
9. Yanagida, S., et al., Catalysts, 2019. **9**(1): p. 82.
10. Aubry, E., et al., Surface and Coatings Technology, 2007. **201**(18): p. 7706-7712.
11. Kuznetsova, A., et al., Glass Physics and Chemistry, 2018. **44**(1): p. 41-46.
12. Zhang, Y., et al., Journal of the European Ceramic Society, 2019. **39**(15): p. 4891-4900.
13. Ertuş, E.B., C. Vakifahmetoglu, and A. Öztürk, Ceramics International, 2020. **46**(4): p. 4947-4951.
14. Thommes, M., et al., Pure and Applied Chemistry, 2015. **87**(9-10): p. 1051-1069.
15. Freundlich, H., J. Phys. chem, 1906. **57**(385471): p. 1100-1107.
16. Langmuir, I., Journal of the American Chemical society, 1918. **40**(9): p. 1361-1403.
17. Weber, T.W. and R.K. Chakravorti, AIChE Journal, 1974. **20**(2): p. 228-238.
18. Li, W.C., et al., Chemistry–A European Journal, 2005. **11**(5): p. 1658-1664.
19. Kreisberg, V., V. Rakcheev, and T. Antropova, Glass Physics and Chemistry, 2006. **32**(6): p. 615-622.
20. Toquer, G., et al., Journal of Non-Crystalline Solids, 2011. **357**(6): p. 1552-1557.
21. Lyubavin, M., T. Burkat, and V. Pak, Inorganic Materials, 2008. **44**(2): p. 203-206.
22. Müller, R., et al., Talanta, 2013. **107**: p. 255-262.
23. Lei, S., et al., Carbon, 2006. **44**(10): p. 1884-1890.
24. N. Yuan, H. Cai, T. Liu, Q. Huang, X. Zhang, Adsorpt. Sci. Technol. 2019. **37** 333–348.
25. Khraisheh, M., et al., Water Research, 2005. **39**(5): p. 922-932.